Year: 2008

Planimetric and volumetric glacier changes in the Khumbu Himal, Nepal, since 1962 using Corona, Landsat TM and ASTER data

Bolch, Tobias ; Buchroithner, Manfred F ; Pieczonka, Tino ; Kunert, André

Abstract: Multitemporal space imagery from 1962 (Corona KH-4), 1992 (Landsat TM), 2001 and 2005 (Terra ASTER) was used to investigate the glacier changes in the Khumbu Himal, Nepal. The ice coverage in the investigation area decreased by about 5% between 1962 and 2005, with the highest retreat rates occurring between 1992 and 2001. The debris coverage increased concomitantly with the decrease in total glacier area. The clean-ice area decreased by >10%. Digital terrain model (DTM) generation from the early Corona KH-4 stereo data in this high-relief terrain is time-consuming, and the results still contain some elevation errors. However, these are minor in the snow-free areas with gentle slopes. Thus comparison of the surfaces of the debris-covered glacier tongues based on the Corona DTM and an ASTER DTM is feasible and shows the downwasting of the debris-covered glaciers. The highest downwasting rates, more than 20m (>0.5ma-1), can be found near the transition zone between the active and the stagnant glacier parts of the debris-covered glacier tongues. The downwasting is lower, but still evident, in the active ice areas and at the snout with thick debris cover. All investigated debriscovered glaciers in the study area show similar behaviour. The estimated volume loss for the investigated debris-covered glacier tongues is 0.19km3.

Planimetric and volumetric glacier changes in the Khumbu Himal, Nepal, since 1962 using Corona, Landsat TM and ASTER data

Tobias BOLCH,[*] Manfred BUCHROITHNER, Tino PIECZONKA, André KUNERT

Institut für Kartographie, Technische Universität Dresden, D-01062 Dresden, Germany
E-mail: tobias.bolch@tu-dresden.de

ABSTRACT. Multitemporal space imagery from 1962 (Corona KH-4), 1992 (Landsat TM), 2001 and 2005 (Terra ASTER) was used to investigate the glacier changes in the Khumbu Himal, Nepal. The ice coverage in the investigation area decreased by about 5% between 1962 and 2005, with the highest retreat rates occurring between 1992 and 2001. The debris coverage increased concomitantly with the decrease in total glacier area. The clean-ice area decreased by >10%. Digital terrain model (DTM) generation from the early Corona KH-4 stereo data in this high-relief terrain is time-consuming, and the results still contain some elevation errors. However, these are minor in the snow-free areas with gentle slopes. Thus comparison of the surfaces of the debris-covered glacier tongues based on the Corona DTM and an ASTER DTM is feasible and shows the downwasting of the debris-covered glaciers. The highest downwasting rates, more than 20 m ($>0.5\,\mathrm{m\,a^{-1}}$), can be found near the transition zone between the active and the stagnant glacier parts of the debris-covered glacier tongues. The downwasting is lower, but still evident, in the active ice areas and at the snout with thick debris cover. All investigated debris-covered glaciers in the study area show similar behaviour. The estimated volume loss for the investigated debris-covered glacier tongues is 0.19 km^3.

INTRODUCTION

Glaciers are key indicators for assessing climate change in remote mountain areas where climate stations are rare or non-existent. Since the end of the Little Ice Age, and especially since the end of the last century, a nearly global glacier recession has been noticeable (Barry, 2006). Previous studies also show receding glaciers for most of the Himalaya (Kadota and others, 2000; Fujita and others, 2001; Ren and others, 2006; S.C. Rai, http://assets.panda.org/downloads/himalayaglaciersreport2005.pdf). However, this does not imply a synchronous behaviour of all glaciers, because there can be local differences and even advancing glaciers. Multitemporal spaceborne images are ideal to study glacier changes in detail. In addition, they are the best way to investigate glaciers in remote mountainous areas. Multi-spectral satellite imagery represents an ideal tool for auto-mated glacier mapping. A simple but robust method is the use of ratio image, (e.g. near-infrared/shortwave-infrared (NIR/SWIR) band such as Landsat Thematic Mapper 4 and 5 (TM4/TM5) or Advancesd Spaceborne Thermal Emission and Reflection Radiometer (ASTER) bands 3 and 4 (Paul and others, 2002; Bolch and Kamp, 2006)). However, many glacier tongues in the Himalaya are heavily covered by supraglacial debris (Moribyashi and Higuchi, 1977) which hampers the automated delineation using multi-spectral imagery. A promising approach to map these glacier parts is to include morphometric information (Bolch and others, 2008).

The earliest imagery suitable for automated glacier mapping is available from 1982 from the Landsat 4 (TM) sensor, which was equipped with SWIR bands capable of rapidly distinguishing snow/ice-covered areas from other surfaces. They have, however, no stereo-capability to address volume changes. This is especially needed to address the fluctuation of the debris-covered glaciers, because their change is mainly recognizable through downwasting (Kadota and others, 2000).

Declassified satellite imagery is available for 1960–72 from American intelligence satellite missions. Early systems (Corona KH-1, KH-2, KH-3) carried a single panoramic camera, whereas later systems (KH-4, KH-4A and KH-4B) carried two panoramic cameras with a separation angle of 30°. For KH-4 (resolution <8 m), KH-4A and KH-4B (reso-lution ∼2–7 m) the two cameras are referred to as fore (forward-looking) and aft (rear-looking) and provide stereo coverage and the capability to generate digital terrain models (DTM) (Altmaier and Kany, 2002). The ASTER sensor on the Terra satellite, which was launched in 1999, captures stereo images in the NIR band (resolution 15 m) and is therefore also capable of DTM generation. The overall quality of these ASTER DTMs is good, although problems like height inaccuracies can occur, especially in terrain with high relief (Kääb, 2002; Kamp and others, 2005).

The aim of this study is to address the glacier area changes for the Khumbu Himal, Nepal, for different time periods using multitemporal satellite imagery, and to shed light not only on the downwasting of Khumbu Glacier but also on other debris-covered glacier tongues using DTMs from Corona KH-4 (year 1962) and ASTER (year 2002). The presented work is a contribution to the international programme Global Land Ice Measurements from Space (GLIMS) (Kargel and others, 2005).

STUDY AREA

The study area of the Khumbu Himal is situated at the main ridge of the Himalaya, south of Qomolangma (Fig. 1). The climate is influenced by the Indian monsoon, and 70–80% of the precipitation occurs during the summer months (Ueno
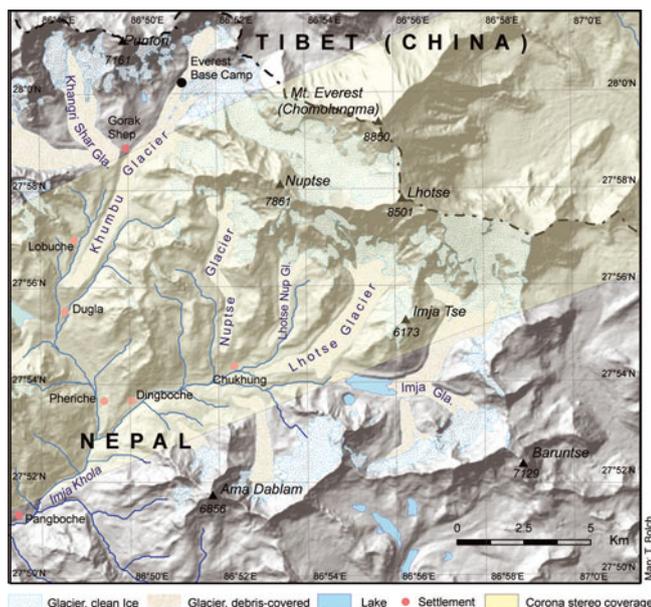
Fig. 1. Map of the study area based on ASTER data from November 2005.

Fig. 2. Eastern margin of Nuptse Glacier with a small secondary moraine (arrow). Photograph: T. Bolch, 2006.

and others, 2001). The glaciers can be classified as 'summer-accumulation-type glaciers' (after Ageta and Higuchi, 1984). Thus, the glaciers are especially sensitive to summer temperature (Kadota and others, 1993). Avalanches are an important feeding source for Khumbu Glacier, and are about twice as significant as direct snowfall (Inoue, 1977).

About one-third of the glaciers in the Khumbu Himal are debris-covered (Fujii and Higuchi, 1977). The thickness of the debris cover of Khumbu Glacier increases towards its terminus and reaches up to several metres. It also increases from the middle of the glacier tongue to the lateral moraines (Nakawo and others, 1986; Watanabe and others, 1986). The termini of the debris-covered glaciers extend down to about 4900 m a.s.l., which is 300–400 m lower than the tongues of the glaciers with clean ice (Moribyashi and Higuchi, 1977).

The end of the active debris-covered glacier tongue is not clearly identifiable and it is likely that the investigated tongues contain parts of stagnant ice at the front which are probably connected with the active glacier ice. However, these stagnant parts differ in their surface characteristics. They are smoother, and locally even sparse grass vegetation is able to grow. These surface features of Khumbu Glacier have been well described (Iwata and others, 1980; Watanabe and others, 1986; Gades and others, 2000). The end of the active glacier tongue is estimated to be about 3 km upstream (Fushimi, 1977; Luckman and others, 2007). The parts of stagnant ice are commonly included in the glacier boundary (e.g. for the Nepalese Glacier Inventory (Mool and others, 2001)). During field surveys, the existence of small secondary moraines has been observed, which indicates vertical surface displacement (Buchroithner and Bolch, 2007; Fig. 2).

Several supraglacial ponds, ice cliffs and thermokarst are typical for these debris-covered tongues with a rough surface. Due to climate change, some of these ponds grow and form a supra- or proglacial lake, such as Imja lake. The formation of the latter has been well described (Watanabe and others, 1995). Even when comparing recent ASTER images of 2003 and 2005, the surface of Imja lake is growing. The danger of an outburst of these lakes (glacial lake outburst flood monitoring and early warning sytem, (GLOF)) is well known and has been the subject of several studies (e.g. Yamada and Watanabe, 1998; Quincey and others, 2007).

Looking at multitemporal space imagery, such as Corona (1962) and ASTER (2003; Fig. 3), at first glance it seems that these debris-covered glaciers are mostly stable. However, the recent glacier shrinkage results in increasing debris coverage and an increasing number and total area of supraglacial lakes. In addition, the surface, especially at the very distal part of the glacier, looks smoother and shows no significant indication of movement, steep ice cliffs or furrows. The latter could be demonstrated using multi-temporal IKONOS and ASTER data or radar data (Luckman and others, 2007). It should be mentioned that a clear delineation of the glacier termini is also not possible, or at least only with a high degree of uncertainty with ultra-high resolution images (e.g. QuickBird, IKONOS) and even field observations. At this point, geophysical investigations seem to be required.

PRESENT KNOWLEDGE OF GLACIER VARIATIONS IN THE KHUMBU HIMAL

The glaciers in the Khumbu Himal, as in most other parts of the Himalaya, show an average area loss and negative mass balances. However, although Khumbu Glacier has been subject to several studies, no comprehensive multitemporal glacier inventory, including recent data, exists thus far for the study area. A comparison of the glacier inventories from 1960 (Müller, 1970) and 1975 reveals a retreat of most glaciers in the Khumbu region, but the area loss has not been quantified (Higuchi and others, 1980). The retreat probably accelerated in the 1980s (Yamada and others, 1992). Observations of the clean-ice glacier AX010, situated in the Shorong Himal southwest of the Khumbu Himal, show that since measurements began in 1978 mass balance has been negative and the mass loss accelerated in the 1990s (Fujita and others, 2001). The area of the same glacier shrunk between 1978 and 1999 from 0.57 to 0.42 km^2 (more than 26%; Fujita and others, 2001). Concomitant with the glacier retreat, the debris-covered areas increase on most of the glaciers (e.g. Khumbu Glacier (Iwata and others, 2000)).
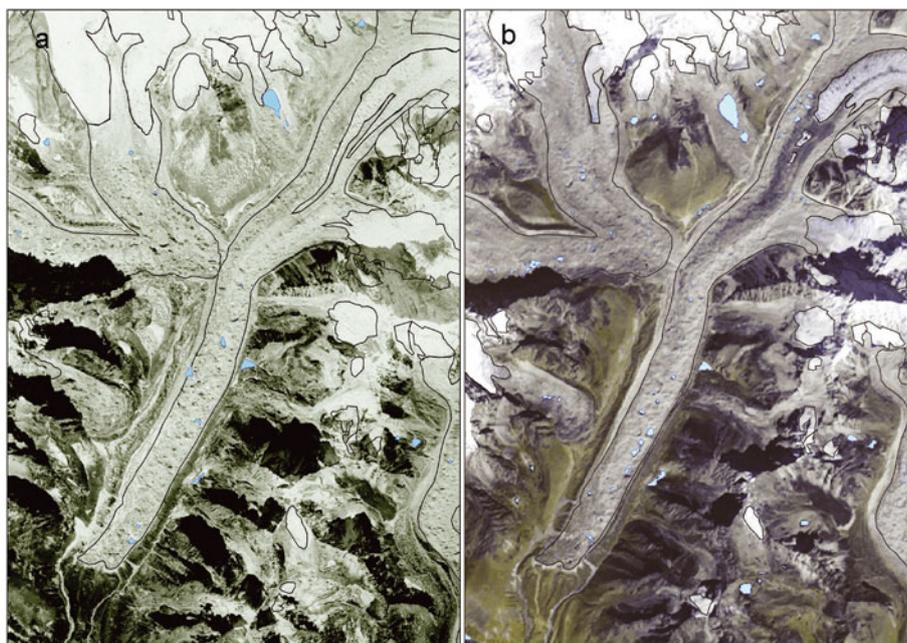
Fig. 3. Khumbu Glacier: (a) Corona image from 1962; (b) ASTER image from 2003. Black lines represent the glacier outlines and the transition between the debris-covered and clean-ice glacier; lakes are represented in light blue.

The change in debris-covered glacier tongues is mostly noticeable through downwasting, because the termini are often either more-or-less constant or the terminus change is not identifiable due to the massive debris cover. Nakawo and others (1999) calculated an average rate of 1–2 m a^{-1} around the Everest Base Camp for Khumbu Glacier from flow velocity, glacier surface temperature estimates based on satellite data and glacier thickness estimates. The melt rate is lowest (close to zero) at about 4 km down-glacier from Everest Base Camp, where the debris cover is thick and the movement rate still high. Melt rate is highest ($\sim$1.5 m a^{-1}) at the estimated transition zone between active and inactive glacier parts. We assume a slight surface lowering at the stagnant glacier part with thick debris cover. The reason for the high ablation rates in the debris-covered area is the strong ablation at the ice cliffs and around the supraglacial lakes (Inoue and Yoshida, 1980; Sakai and others, 2000). A detailed comparison based on surface measurements between 1978 and 1995 also shows melt rates of 0.4–1.0 m a^{-1}. The highest rates were measured at the places with thin debris cover and at the transition zone between the active and inactive glacier tongue (Kadota and others, 2000). Between 1995 and 1999 the ablation rates doubled at the investigated surfaces around the Everest Base Camp, at the estimated transition zone between thin debris cover and clean ice and also in areas

with thick debris cover (Kadota and others, 2002). Detailed comparisons of the surface of Khumbu Glacier between 1978 and 1995 show that the areas with rough surface have increased both upwards and downwards of the transition zone. Therefore the areas with high ablation rates also increased. This is one reason for the higher rates of downwasting (Iwata and others, 2000). However, the parts with stagnant ice remained about the same.

Owing to the high melting rates, Nakawo and others (1999) assume that large parts of the glacier tongue will disappear in about 100 years. A simulation of the Khumbu Glacier tongue predicts the development of a depression in the year 2020 and the splitting of the ablation area into two unconnected parts after 2040: the stagnant ice area and the active ice, possibly with a lake in between (Naito and others, 2000). A recent study of the glaciers on the north side of Qomolangma indicates similar behaviour, at least since the start of investigations in 1966 (Ren and others, 2006).

DATA AND METHODS

Imagery

Multitemporal and low-cost data from different sensors were applied to assess glacier change in the Khumbu Himal. The oldest data originate from the American Corona KH-4 sensor (1962) and the youngest from the ASTER sensor on board the Terra satellite (2005; see Table 1). Two ASTER scenes (2001 and 2005) were chosen. These scenes cover the Khumbu Himal and are, for the main area of interest, nearly cloud-free. The basis for georectification was the map 'Mount Everest' published in 1988 by the US National Geographic Society (NGS, 1988). Unfortunately, this map does not cover the whole area to the mountain ridges west of Khumbu Glacier, so this region had to be excluded. About 100 ground-control points (GCPs) were chosen for rectification purposes for each ASTER scene. Orthoimages were generated using the ASTER DTM (see below). The overall RMS$_{x,y}$

Table 1. Remote-sensing data used

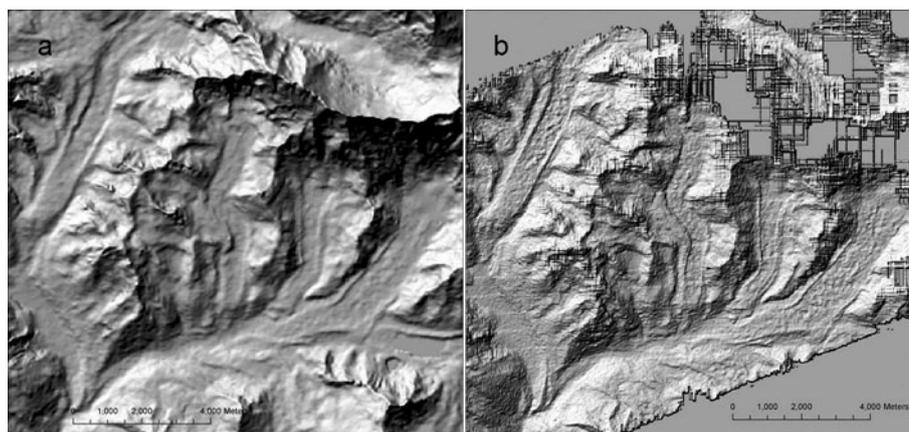| Date	Sensor	Image information	Resolution	Accuracy RMS$_{x,y}$
15 Dec 1962	Corona KH-4	Panchromatic	8 m	$\sim$15 m
17 Nov 1992	Landsat TM	Multispectral	30 m	<50 m
20 Dec 2001	Terra ASTER	Multispectral	15 m	<15 m
29 Nov 2005	Terra ASTER	Multispectral	15 m	<15 m

Fig. 4. Comparison of (a) the ASTER-derived DTM from ~2002 and (b) the Corona-derived DTM from 1962, including the surface of several debris-covered glaciers.

error was less than one pixel (15 m; Table 1), despite the high relief differences. In addition, a cloud-free Landsat TM scene of 1992 obtained by the Global Land Cover Facility (GLCF) was referenced to these ASTER data. The accuracy is lower than that of the ASTER data (with higher resolution) but still acceptable (Table 1). The higher $RMS_{x,y}$ results are mainly due to deviations around high mountain ridges and peaks. Three Corona strips were required to provide a cloud-free cover of the whole study area, while the snow cover was acceptable. The main disadvantage is the low contrast in the snow-covered areas which hampers glacier mapping. However, the lower glacier boundaries are identifiable when image-stretching procedures are applied. The $RMS_{x,y}$ error is in the range of the ASTER data.

DTM generation and evaluation

For the ASTER DTM of the investigation area, a subset was drawn around Qomolangma containing all the debris-covered glaciers originating at Qomolangma, Lhotse and Nuptse. The DTM is based on scenes from 2001, 2002 and 2003. Using 18 GCPs determined on the basis of the Qomolangma map (NGS, 1988) and approximately 100 tie points for each scene, a DTM was generated from each stereo pair using the PCI Geomatica 9.1 software. The raw DTMs contained several data gaps, mainly situated at steep slopes, in shadowed areas and in snow-covered areas. In contrast, the valleys, including the debris-covered glacier tongues, are well represented. In post-processing steps, the three DTMs were combined and the remaining data gaps were filled with terrain information derived from the NGS map (Buchroithner and Bolch, 2007). The quality of the final DTM is promising (Fig. 4a).

In order to assess the accuracy, 205 independent control points covering non-glaciated areas of the whole DTM were used and compared with elevations based on the NGS map.

Shuttle Radar Topography Mission (SRTM) data were not used for quality control because of the coarser resolution of 90 m. The calculated RMS_z error of the SRTM data was 80.6 m. In order to calculate the error near the glaciers, the areas of the control points were reduced to a buffer area of 500 m around the glacier tongues. The error analysis shows that the ASTER DTM is too low on average, with an RMS_z error of about 30 m. However, the accuracy is acceptable given the very steep slopes and the high relief differences of up to 5000 m. In addition, the RMS_z error is significantly smaller in the areas around the glacier tongues (Table 2). However, the single ASTER DTMs are too coarse to recognize the expected glacier downwasting between 2001 and 2003.

The Corona DTM is based on one forward-looking and one aft-looking strip of the KH-4 sensor. Most of the target area is covered in both scenes and is situated near the centre of the images. The contrast is good, apart from the snow-covered higher elevations at Qomolangma, Lhotse and Nuptse and the steep slopes situated in the shadows. The most challenging tasks of these Corona data are caused by their complex image geometry. Also, especially during this early mission, the flight and acquisition parameters were very unstable. Therefore, image parameters have to be estimated. The RSG software (Remote Sensing Software Package Graz), which is an add-on to ERDAS Imagine, has a tool especially developed to estimate the Corona image parameters using GCPs. The sources for the >100 GCPs for the Corona DTM of the Qomolangma area were the NGS map and the orthorectified ASTER scenes. The same GCPs as for the ASTER DTM were used if they were identifiable in the Corona image. For the outer parts of the 200 km long Corona strips, where no other data were available (especially in Tibet), orthorectified Landsat Enhanced TM Plus (ETM+)-scenes downloaded from GLCF were used. The latter had to be included to calculate the camera position.

Table 2. Resolution and accuracy of the raw Corona and ASTER DTMs

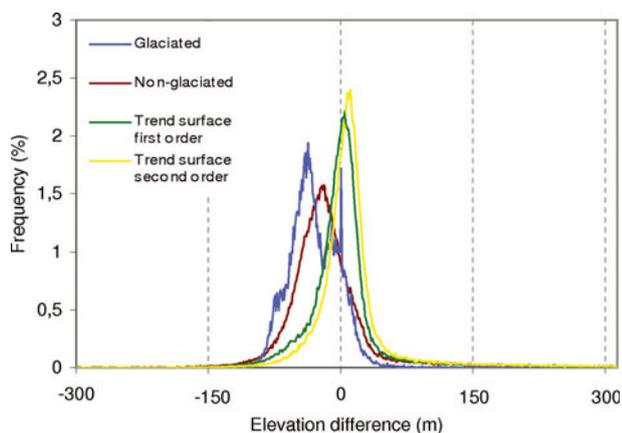| Sensor	Resolution	$RMS_{x,y}$	Mean elevation difference	RMS_z (whole DTM)	RMS_z (buffer of 500 m around the debris-covered glaciers)
Terra ASTER	30 m	<1 pixel (30 m)	−8.1 m	29.3 m	14.8 m
Corona KH-4	20 m	<1 pixel (20 m)	−26.0 m	56.5 m	18.0 m

Fig. 5. Histogram of the height differences between ASTER and Corona DTM.

Besides these coarse data for the outer parts of the image strips, the *x,y* accuracy in the target area is <20 m (Table 1). Shape and surface characteristics, in particular the glacier surfaces, are better represented in the Corona DTM than in the ASTER DTM (Fig. 4b). This is also due to the higher resolution (20 vs 30 m). However, the Corona DTM has many data gaps and large elevation errors on the steep slopes and snow-covered mountain ridges. On average, this DTM is too low. A further problem is that the northwestern areas tend to be too high and the southeastern areas too low. This may be due to an unstable camera during image acquisition. Also, in the southeastern areas of the Corona image, fewer GCPs could be identified because of high snow cover and low contrast. The overall RMS_z error (>50 m) is therefore relatively high. However, as with the ASTER DTM, the errors in the area of interest are much less (Table 1) and the glacier surfaces are well represented (Fig. 4b). In addition, the relative accuracy (rather than the absolute accuracy) of the DTMs is most important for addressing glacier volume change. Figure 5 is a histogram of the frequency distribution of the height differences between the two DTMs. The mean elevation of the glaciated areas is lower than for the non-glaciated areas.

In order to minimize systematic height errors, a first- and second-order trend surface were calculated based on the non-glaciated surface at elevations between 4500 and 5500 m a.s.l. where the debris-covered glaciers and their moraines are situated. Correction by these trend surfaces leads to significant improvements. The mean elevation difference is only about 3 m, the frequency distribution is higher and narrower (Fig. 5) and the RMS_z is lower (Table 3). The first-order trend correction is slightly better than the
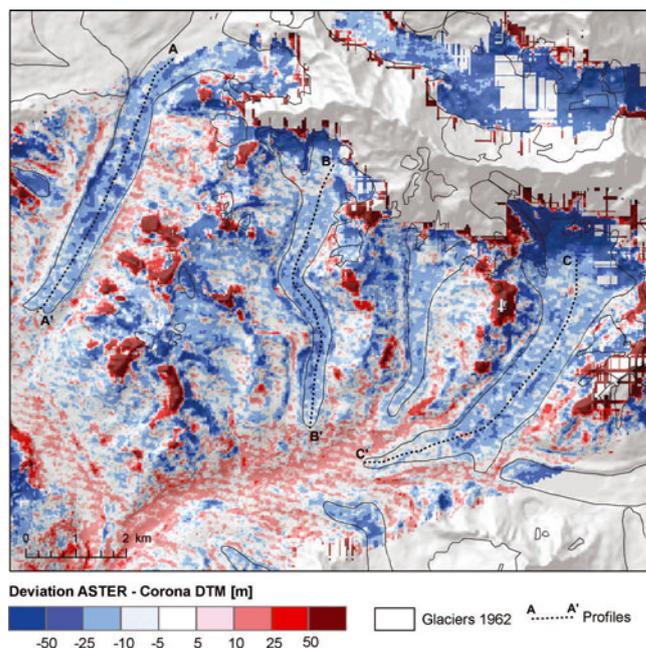

Fig. 6. Difference between the surface elevations of Khumbu Glacier based on ASTER and Corona DTMs. Areas with no Corona DTM coverage or where the DTM generation failed are represented by the shaded ASTER DTM. For the profiles see Figure 7.

second-order trend correction. In order to estimate the error at the debris-covered glacier tongues, statistics for all areas with similar surface slope conditions to those at the tongues (0–25°) within a 500 m buffer around those tongues were calculated and analyzed. The mean elevation difference between the improved Corona DTM and the ASTER DTM is 0.7 m with a standard deviation of 9.6 m. These statistics vary slightly for each glacier (Table 3).

The height difference between the ASTER and the Corona DTM is shown in Figure 6. Obvious errors with deviations up to 300 m occur at the steep slopes (e.g. at the accumulation area of Lhotse Glacier and the headwall above), snow-covered peaks and areas of higher elevation (e.g. the mountain ridges between the debris-covered glaciers).

The elevation differences in the valleys and on gentle slopes rarely exceed 25 m and are mostly positive, whereas the differences are clearly negative at all glacier tongues. It seems there is also a surface lowering at the accumulation area of Khumbu Glacier. However, as nearly stable areas in the surrounding parts are at very steep slopes where the DTM generation failed, an error analysis cannot be performed. The large differences (>50 m) between Qomolangma, Lhotse and Nuptse are likely an error of the DTMs.

Table 3. Relative accuracy of the Corona and ASTER DTMs for the whole non-glaciated areas and for a buffer of 500 m around the debris-covered glacier tongues

	Without trend	First-order trend	Second-order trend	Buffer without trend	Buffer first-order trend (min, max)
	m	m	m	m	m
Mean	−13.9	2.9	11.3	−9.3	0.7 (−3.9, 5.2)
Standard deviation	51.4	48.3	46.9	18.9	9.6 (8.6, 10.0)
RMS_z	53.2	48.4	48.2	n.c.	n.c.

n.c.: not calculated.

Table 4. Changes of total ice cover, the clean-ice and debris-covered ice areas in the Khumbu Himal between 1962 and 2005 based on spaceborne imagery

Year (sensor)	Ice extent			Period	Change rate			% change rate		
	Total area	Clean ice	Debris cover		Total area	Clean ice	Debris cover	Total area	Clean ice	Debris cover
	km^2	km^2	km^2		$km^2 \, a^{-1}$	$km^2 \, a^{-1}$	$km^2 \, a^{-1}$	$\% \, a^{-1}$	$\% \, a^{-1}$	$\% \, a^{-1}$
1962 (Corona)	92.26	56.54	35.73	1962–2005	−0.11	−0.13	+0.02	−0.12	−0.24	+0.06
1992 (Landsat TM)	89.69	54.63	35.05	1962–92	−0.086	−0.064	−0.023	−0.09	−0.11	−0.06
2001 (ASTER)	87.64	51.59	36.05	1992–2001	−0.228	−0.338	+0.111	−0.25	−0.62	+0.32
2005 (ASTER)	87.39	50.8	36.60	2001–05	−0.11	−0.13	+0.02	−0.12	−0.24	+0.06

Glacier mapping

The main difficulties for automated glacier mapping are the high percentage of debris-covered glacier tongues and the often not clearly defined accumulation zones. The reasons for the latter are the extremely steep slopes where snow and ice can only accumulate in some areas, and the fact that many of the larger areas are fed mainly by avalanches. In addition, the highest parts of the mountains (above 6000–6500 m) are snow-covered in all scenes. Hence, all tested methods, such as image ratios, the normalized-difference snow index (NDSI) and a supervised classification, overestimate the accumulation zones. A reasonable estimation in the higher regions where many ice masses are situated is provided by the slope gradient, since the accumulation of glacier ice is dependent on the slope. The above-mentioned automated mapping approaches using thermal and morphometric information for the debris-covered glacier parts (Bolch and others, 2008) are very useful to detect debris-covered glaciers and roughly to estimate their size. However, the inaccuracy is in the range of 5%. Therefore, these features are only suitable to estimate larger changes. The best way to address glacier change as accurately as possible is still by manual delineation. This should be done preferably by one expert, so that the delineation, especially in the accumulation zone and the debris-covered glacier parts, is consistent.

Owing to the different resolution of the scenes used, the x, y deviation and the difficulties in clearly identifying glaciers led to errors. The error range was estimated based on a comparison between manually delineated glaciers from a high-resolution IKONOS scene (merging the panchromatic data (resolution 1 m) and the multispectral data (resolution 4 m)) and an ASTER scene. The approximate error amounts to 2%, highest when comparing the Corona data with Landsat and lowest between the two ASTER scenes. All debris-covered ice areas, whether active or inactive, are included in the glacier area. The terminus of Imja Glacier was drawn at the proximal end of the lake, despite the fact that ice might exist under certain parts of the lake.

RESULTS
Glacier area changes

The overall ice-covered area in the Khumbu Himal (comparing Khumbu, Nuptse and Lhotse glaciers) decreased between 1962 and 2005 by 5.3 ± 2% (~0.12% a^{-1}; Table 4). The highest area loss can be found from 1992 to 2001 (~0.25% a^{-1}) and the lowest between 1962 and 1992 (~0.09% a^{-1}). The area loss seems to slow down, but this

is not a significant trend due to the short period of 4 years (2001–05) and the small amount, which barely exceeds the error range. The debris-covered ice area increased significantly between 1962 and 2005, by nearly 2.5% (0.06% a^{-1}), despite the fact that the growing Imja lake, which formed after 1962, was totally excluded from Imja Glacier.

It should also be mentioned that, according to the local people (Nakawo and others, 1999), the increase of the debris cover in the pinnacle zone near the Everest Base Camp is partly due to a landslide. However, this area is comparatively small and does not affect the overall trend. The increase of the debris-covered areas is mainly due to the decrease of the clean-ice areas in the transition zone between clean and debris-covered glacier (Fig. 3). Accordingly, the clean-ice area decreased more than 10% (0.24% a^{-1}) between 1962 and 2005 (Table 4). The loss of the clean-ice areas was highest between 1992 and 2001 and lowest between 1962 and 1992.

Surface lowering

The values in Table 4 clearly show the importance of addressing the changes in the debris-covered areas in more detail. Existing investigations of the downwasting of debris-covered glacier tongues in the study area have concentrated on Khumbu Glacier, and are based only on point measurements or estimations. In order to address the volume changes, the Corona DTM (1962) and the ASTER DTM (2002) of Khumbu, Nuptse, Lhotse Nup and Lhotse glaciers were compared. Unfortunately, only about 50% of the ablation zone of Khumbu Glacier is covered by the Corona DTM (Fig. 1), and statistics refer only to this covered part.

A downwasting from about 11 m (Lhotse Glacier) to nearly 17 m on average (Khumbu Glacier) can be measured for all four glaciers (Table 5). However, the average downwasting exceeds the estimated errors clearly for only Khumbu Glacier, and is a little lower than the average DTM difference for Lhotse Glacier. Taking into account that the mean elevation of the surroundings for Lhotse Glacier is 5.2 m higher than for the ASTER DTM, there is still strong evidence for the downwasting of this glacier. In addition, the errors are less than the expected downwasting rates of more than 20 m, taking the results presented thus far for Khumbu Glacier into account (Kadota and others, 2002). Therefore, the use of these DTMs is suitable to address the glacier downwasting.

Each glacier contains larger areas where the elevation difference between the ASTER and the Corona DTM is higher than 25 m. This is also confirmed with the length profiles. These profiles indicate that all debris-covered glacier tongues

Table 5. Calculated downwasting and volume loss of the investigated debris-covered glacier tongues

Glacier	Mean height difference of glacier surroundings	Average downwasting	Average downwasting rate	Volume loss
	m	m	m a^{-1}	m^3
Khumbu (covered part)	+2.4	−16.9 ± 8.6	0.42 ± 0.21	(68.1 × 10^6) ± (34.6 × 10^6)
Nuptse	−3.9	−13.7 ± 9.7	0.34 ± 0.24	(43.2 × 10^6) ± (30.5 × 10^6)
Lhotse Nup	−1.1	−11.4 ± 9.9	0.29 ± 0.25	(18.0 × 10^6) ± (15.6 × 10^6)
Lhotse	+5.2	−10.8 ± 10.0	0.27 ± 0.25	(62.8 × 10^6) ± (58.1 × 10^6)
Sum/average	+0.7	−13.3 ± 9.6	0.33 ± 0.24	(192.1 × 10^6) ± (138.7 × 10^6)

show similar behaviour (Fig. 7), i.e. a slight downwasting at the glacier snouts where the glaciers are presumably stagnant (e.g. Khumbu and Lhotse up to 2 km, Nuptse up to 1 km from terminus; average downwasting 5–15 m or 0.12–0.37 m a^{-1}). The downwasting is clearly pronounced in the middle part of the glaciers, where the transition zone between the active and inactive glacier parts might be situated (Khumbu, Lhotse 2–3 km, Nuptse 1.0–2.5 km from the terminus). Here, the average downwasting is >20 m (0.5 m a^{-1}), with maxima exceeding 50 m (1.25 m a^{-1}). The downwasting is less pronounced again in the upper highly debris-covered but presumably active part of the glacier. The average downwasting rates are similar to those at the snout. The clearly visible peaks in the length profiles and areas where the ASTER DTM showed higher elevation values than the Corona DTM are most probably due to the different locations of prominent thermokarst formations and supraglacial ponds or inaccuracies in the DTMs.

DISCUSSION

The use of multitemporal space imagery for glacier monitoring is well known. Although the image geometry of the Corona images is very complex and the image processing and rectification is time-consuming, the data are of tremendous use in giving more insight into glacier changes since the early 1960s. This is mainly due to the high resolution (<10 m) and stereo capability. Moreover, these data are available for many remote mountain areas where no aerial images are available or accessible.

It could be demonstrated that Corona-based DTMs are suitable for comparative studies of glacier volumes. This study is one of the first presenting results using the early KH-4 stereo data with a resolution of about 8 m. Previously presented results, which were more accurate in elevation, made use of later KH-4A and KH-4B data with higher resolution (Altmaier and Kany, 2002).

The areal changes of the glaciers in the Khumbu Himal confirm the expected and widely published overall glacier retreat, but also quantify and give insight into the differences in the debris-covered and clean-ice areas for different times within the last 45 years. The pronounced glacier retreat in the 1990s shows behaviour similar to that of the well-investigated glacier AX10 (Fujita and others, 2001). Whether the less pronounced shrinkage at the beginning of the 21st century represents a stable trend needs further investigation. The use of suitable remote-sensing data from the early 1980s (such as aerial photographs from the NGS survey) would give even more insight into glacier change and would

probably confirm the beginning of the pronounced glacier retreat in the 1980s (evidence based on ground surveys; Yamada and others, 1992) of selected glaciers. The present study also confirms the assumption that concomitantly with the glacier retreat, the debris-covered areas increase not only on Khumbu Glacier (Iwata and others, 2000) but also on all other glaciers in the investigation area.

The calculation of the surface lowering based on the Corona and ASTER DTMs certainly contains errors due to the uncertainties of the DTMs. However, the characteristics of the surface changes are very well represented, and the calculated lowering rates for Khumbu Glacier are in agreement with the estimates of Nakawo and others (1999) and Kadota and others (2000). Kadota and others (2000) measured the surface changes between 1978 and 1995 to be 10–14 m (0.6–0.8 m a^{-1}) about 3 km upstream of the terminus. The calculated average downwasting between 1962 and 2002 based on the ASTER and Corona DTMs of the same area is ∼20 m (∼0.5 m a^{-1}). The study also confirms the lower but still evident downwasting rates in the heavily debris-covered active ice areas and the snout with thick debris cover. In addition, the DTM comparison sheds light on the characteristics of the downwasting not only of Khumbu Glacier but also, for the first time, of Lhotse, Lhotse Nup and Nuptse glaciers. The overall volume loss from the investigated glaciers is less than reported for debris-covered glacier tongues in the western Himalaya (Berthier and others, 2007), but is still significant.

The findings concerning glacier recession and downwasting are important not only in improving knowledge about glacier water resources and the contribution of Himalayan glaciers to sea-level rise, but also in assessing preglacial and supraglacial lake development for the risk of outburst flood. The downwasting of the investigated debris-covered glaciers is pronounced about 1–3 km upstream of the terminus in an area where the transition between the active and the stagnant ice is expected. This can lead to a depression which is likely to be filled by a glacial lake (e.g. for Khumbu and Nuptse Glaciers with flat termini) and confirms the simulation by Naito and others (2000) for Khumbu Glacier. In contrast, the development of a large lake is less probable for Lhotse Glacier, due to less pronounced downwasting and especially due to the steeper terminus (Quincey and others, 2007).

CONCLUSIONS

This study, based on multitemporal space imagery from 1962, 1992, 2001 and 2005, shows an average area loss
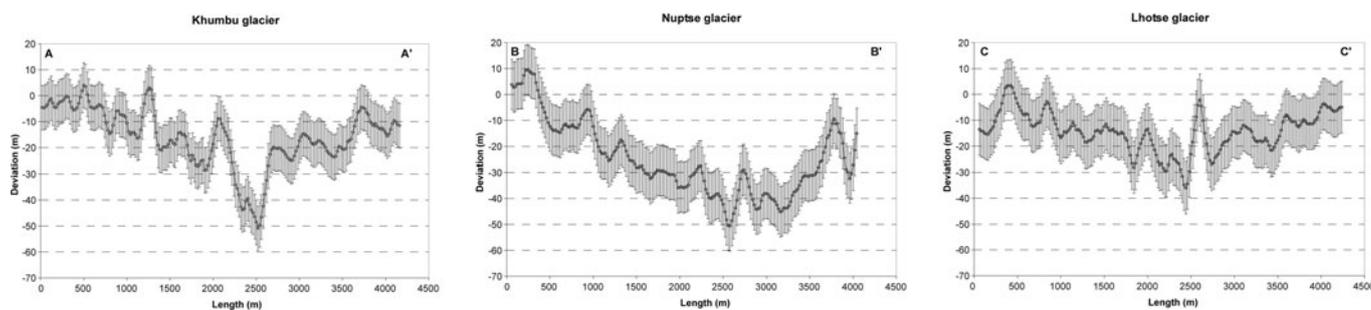
Fig. 7. Length profiles of Khumbu, Lhotse and Nuptse glaciers showing the deviation of the 2002 ASTER DTM and the 1962 Corona DTM which indicates the thickness changes. For the location of these profiles see Figure 5.

from the glaciers in the Khumbu Himal of about 5%. The highest retreat rates are found between 1992 and 2001. The coverage of the glaciers with debris increased concomitantly with a decrease in total glacier area.

The DTM generation from the early Corona KH-4 stereo data in this type of high-relief terrain is difficult and time-consuming, and still contains some elevation errors. Nevertheless, it was shown that DTMs based on space imagery are suitable for monitoring debris-covered glaciers, and a comparison of DTMs demonstrated glacier downwasting. The estimated volume loss for the investigated debris-covered glacier tongues is $0.19 \, \text{km}^3$ over the period 1962–2002. The highest downwasting rates (e.g. $>0.5 \, \text{m a}^{-1}$ for Khumbu Glacier) can be found in the expected transition zones between the active and the stagnant glacier parts of the debris-covered glacier tongue about 1–3 km upstream of the terminus. This may lead to the development of glacial lakes.

Existing and forthcoming sensors and data with stereo capabilities and resolutions of about 2.5 m, such as the optical advance Land Observing Satellite (ALOS), Cartosat and Terra-SAR-X, will provide more insight into the behaviour of debris-covered glaciers.

REFERENCES

Ageta, Y. and K. Higuchi. 1984. Estimation of mass balance components of a summer-accumulation type glacier in the Nepal Himalaya. *Geogr. Ann.,* **66A**(3), 249–255.

Altmaier, A. and C. Kany. 2002. Digital surface model generation from CORONA satellite images. *ISPRS J. Photogramm. Rem. Sens.,* **56**(4), 221–235.

Barry, R.G. 2006. The status of research on glaciers and global glacier recession: a review. *Progr. Phys. Geogr.,* **30**(3), 285–306.

Berthier, E., Y. Arnaud, R. Kumar, S. Ahmad, P. Wagnon and P. Chevallier. 2007. Remote sensing estimates of glacier mass balances in the Himachal Pradesh (Western Himalaya, India). *Remote Sens. Environ.,* **108**(3), 327–338.

Bolch, T. and U. Kamp. 2006. Glacier mapping in high mountains using DEMs, Landsat and ASTER data. *In Proceedings of the 8th International Symposium on High Mountain Remote Sensing Cartography, 20–27 March 2005, La Paz, Bolivia.* Graz, Universitat Graz. Institut für Geographie und Raumforschung 13–24. (Grazer Schriften der Geographie und Raumforschung 41.)

Bolch, T., M.F. Buchroithner, A. Kunert, and U. Kamp. 2008. Automated delineation of debris-covered glaciers based on ASTER data. In Gomarasca, M.A., *ed. Geoinformation in Europe. proceedings of the 27th EARSeL Symposium, 4–7 July 2007.* Bozen, Italy Rotterdam, Millpress, 403–410.

Buchroithner, M.F. and T. Bolch. 2007. An automated method to delineate the ice extension of the debris-covered glaciers at Mt. Everest based on ASTER imagery. *In Proceedings of the 9th International Symposium on High Mountain Remote Sensing Cartography, 14–22 September 2006, Graz, Austria.* 13–24. (Grazer Schriften der Geographie und Raumforschung 43.)

Fujii, Y. and K. Higuchi. 1977. Statistical anayses of the forms of the glaciers in Khumbu region. *Seppyo, J. Jpn. Soc. Snow Ice,* **39**, Special Issue, 7–14.

Fujita, K., T. Kadota, B. Rana, R.B. Kayastha and Y. Ageta. 2001. Shrinkage of Glacier AX010 in Shorong region, Nepal Himalayas in the 1990s. *Bull. Glaciol. Res.* 18, 51–54.

Fushimi, H. 1977. Structural studies of glaciers in the Khumbu region. *Seppyo, J. Jpn. Soc. Snow Ice,* **39**, Special Issue, 30–39.

Gades, A., H. Conway, N. Nereson, N. Naito and T. Kadota. 2000. Radio echo-sounding through supraglacial debris on Lirung and Khumbu Glaciers, Nepal Himalayas. *IAHS Publ.* 264 (Symposium at Seattle 2000 – *Debris-Covered Glaciers*), 13–22.

Higuchi, K. *and 8 others.* 1980. Glacier inventory in the Dudh Kosi region, east Nepal. *IAHS Publ.* 126 (Workshop at Reideralp 1978 – *World Glacier Inventory*), 95–103.

Inoue, J. 1977. Mass budget of Khumbu Glacier. *Seppyo, J. Jpn. Soc. Snow Ice,* **39**, Special Issue, 15–19.

Inoue, J. and M. Yoshida. 1980. Ablation and heat exchange over the Khumbu glacier. *Seppyo, J. Jpn. Soc. Snow Ice,* **41** Special Issue, 26–33.

Iwata, S., O. Watanabe and H. Fushimi. 1980. Surface morphology in the ablation area of the Khumbu glacier. *Seppyo, J. Jpn. Soc. Snow Ice,* **41**, Special Issue, 9–17.

Iwata, S., T. Aoki, T. Kadota, K. Seko, and S. Yamaguchi. 2000. Morphological evolution of the debris cover on Khumbu Glacier, Nepal, between 1978 and 1995. *IAHS Publ.* 264 (Symposium at Seattle, 2000 – *Debris-Covered Glaciers*), 3–11.

Kääb, A. 2002. Monitoring high-mountain terrain deformation from repeated air- and spaceborne optical data: examples using digital aerial imagery and ASTER data. *ISPRS J. Photogramm. Rem. Sens.,* **57**(1–2), 39–52.

Kadota, T., K. Seko, and Y. Ageta. 1993. Shrinkage of glacier AX010 since 1978, Shorong Himal, east Nepal. *IAHS Publ.* 218 (Symposium at Kathmandu 1992 – *Snow and Glacier Hydrology*), 145–154.

Kadota, T., K. Seko, T. Aoki, S. Iwata, and S. Yamaguchi. 2000. Shrinkage of the Khumbu Glacier, east Nepal from 1978 to 1995. *IAHS Publ.* 264 (Symposium at Seattle 2000 – *Debris-Covered Glaciers*), 235–243.

Kadota, T., N. Naito and H. Conway. 2002. Some shrinking features in the uppermost ablation area of the Khumbu Glacier, east Nepal, 1995–1999. *Bull. Glaciol. Res.,* 19, 37–40.

Kamp, U., T. Bolch and J.A. Olsenholler. 2005. Geomorphometry of Cerro Sillajhuay, Chile/Bolivia: comparisons of DEMs derived from ASTER remote sensing data and contour maps. *Geocarto Int.,* **20**(1), 23–34.

Kargel, J.S. *and 16 others*. 2005. Multispectral imaging contributions to global land ice measurements from space. *Remote Sens. Environ.,* **99**(1–2), 187–219.

Luckman, A., D.J. Quincey and S. Bevan. 2007. The potential of satellite radar interferometry and feature tracking for monitoring flow rates of Himalayan glaciers. *Remote Sens. Environ.,* **111**(2–3), 172–181.

Mool, P.K., S.R. Bajracharya and S.P. Joshi. 2001. *Inventory of glaciers, glacial lakes and glacial lake outburst floods: monitoring and early warning systems in the Hindu Kush–Himalayan region, Nepal.* Kathmandu, International Centre for Integrated Mountain Development.

Moribayashi, S. and K. Higuchi. 1977. Characteristics of glaciers in Khumbu region and their recent variations. *Seppyo, J. Jpn. Soc. Snow Ice,* **39**, Special Issue, 3–6.

Müller, F. 1970. A pilot study for an inventory of the glaciers in the eastern Himalayas: inventory of glaciers in the Mount Everest region. *In Perennial ice and snow masses: a guide for compilation and assemblage of data for a world inventory.* Paris, UNESCO/International Association of Scientific Hydrology, 47–59. (Technical Papers in Hydrology 1)

Naito, N., M. Nakawo, T. Kadota and C.F. Raymond. 2000. Numerical simulation of recent shrinkage of Khumbu Glacier, Nepal Himalayas. *IAHS Publ.* 264 (Symposium at Seattle 2000 – *Debris-Covered Glaciers*), 245–254.

Nakawo, M., S. Iwata, O. Watanabe and M. Yoshida. 1986. Processes which distribute supraglacial debris on the Khumbu Glacier, Nepal Himalaya. *Ann. Glaciol.,* **8**, 129–131.

Nakawo, M., H. Yabuki and A. Sakai. 1999. Characteristics of Khumbu Glacier, Nepal Himalaya: recent changes in the debris-covered area. *Ann. Glaciol.,* **28**, 118–122.

National Geographic Society (NGS). 1988. *Mount Everest – Sargarmatha (Nepali) – Qomolanga (Chinese).* (Scale 1 : 50 000). Washington, DC, National Geographic Society.

Paul, F., A. Kääb, M. Maisch, T. Kellenberger and W. Haeberli. 2002. The new remote-sensing-derived Swiss glacier inventory. I. Methods. *Ann. Glaciol.,* **34**, 355–361.

Quincey, D.J. *and 6 others*. 2007. Early recognition of glacial lake hazards in the Himalaya using remote sensing datasets. *Global Planet. Change,* **56**(1–2), 137–152.

Ren, J., Z. Jing, J. Pu and X. Qin. 2006. Glacier variations and climate change in the central Himalaya over the past few decades. *Ann. Glaciol.,* **43**, 218–222.

Sakai, A., N. Takeuchi, K. Fujita, and M. Nakawo. 2000. Role of supraglacial ponds in the ablation process of a debris-covered glacier in the Nepal Himalayas. *IAHS Publ.* 264 (Symposium at Seattle 2000 – *Debris-Covered Glaciers*), 119–130.

Ueno, K. *and 11 others*. 2001. Meteorological observations during 1994–2000 at the automatic weather station (GEN AWS) in Khumbu region, Nepal Himalayas. *Bull. Glaciol. Res.,* 18, 23–30.

Watanabe, O., S. Iwata and H. Fushimi. 1986. Topographic characteristics in the ablation area of the Khumbu Glacier, Nepal Himalaya. *Ann. Glaciol.,* **8**, 177–180.

Watanabe, T., S. Kameyama and T. Sato. 1995. Imja Glacier dead-ice melt rates and changes in a supra-glacial lake, 1989–1994, Khumbu Himal, Nepal: danger of lake drainage. *Mt. Res. Dev.,* **15**(4), 292–300.

Yamada, T. and O. Watanabe, *eds*. 1998. *Glacier lake and its outburst flood in the Nepal Himalaya.* Tokyo, Japanese Society of Snow and Ice. Data Center for Glacier Research.

Yamada, T. *and 7 others*. 1992. Fluctuations of the glaciers from the 1970s to 1989 in the Khumbu, Shorong and Langtang regions, Nepal Himalayas. *Bull. Glacier Res.* 10, 11–19.